

# A Small Multifunctional Pentatricopeptide Repeat Protein in the Chloroplast of *Chlamydomonas reinhardtii*

Abdullah Jalal<sup>1</sup>, Christian Schwarz<sup>1</sup>, Christian Schmitz-Linneweber<sup>2</sup>, Olivier Vallon<sup>3</sup>, Jörg Nickelsen<sup>1</sup> and Alexandra-Viola Bohne<sup>1,\*</sup>

<sup>1</sup>Molecular Plant Sciences, Ludwig-Maximilians-University, Grosshaderner Straße 2–4, 82152 Planegg-Martinsried, Germany

<sup>2</sup>Molecular Genetics, Institute of Biology, Humboldt University of Berlin, 10115 Berlin, Germany

<sup>3</sup>UMR7141 CNRS/Université Pierre et Marie Curie, Institut de Biologie Physico-Chimique, 13 Rue Pierre et Marie Curie, 75005 Paris, France

\*Correspondence: Alexandra-Viola Bohne ([alexandra.bohne@lmu.de](mailto:alexandra.bohne@lmu.de))

<http://dx.doi.org/10.1016/j.molp.2014.11.019>

## ABSTRACT

Organellar biogenesis is mainly regulated by nucleus-encoded factors, which act on various steps of gene expression including RNA editing, processing, splicing, stabilization, and translation initiation. Among these regulatory factors, pentatricopeptide repeat (PPR) proteins form the largest family of RNA binding proteins, with hundreds of members in flowering plants. In striking contrast, the genome of the unicellular green alga *Chlamydomonas reinhardtii* encodes only 14 such proteins. In this study, we analyzed PPR7, the smallest and most highly expressed PPR protein in *C. reinhardtii*. Green fluorescent protein-based localization and gel-filtration analysis revealed that PPR7 forms a part of a high-molecular-weight ribonucleoprotein complex in the chloroplast stroma. RIP-chip analysis of PPR7-bound RNAs demonstrated that the protein associates with a diverse set of chloroplast transcripts *in vivo*, i.e. *rrnS*, *psbH*, *rpoC2*, *rbcl*, *atpA*, *cemA-atpH*, *tscA*, and *atpl-psaJ*. Furthermore, the investigation of PPR7 RNAi strains revealed that depletion of PPR7 results in a light-sensitive phenotype, accompanied by altered levels of its target RNAs that are compatible with the defects in their maturation or stabilization. PPR7 is thus an unusual type of small multifunctional PPR protein, which interacts, probably in conjunction with other RNA binding proteins, with numerous target RNAs to promote a variety of post-transcriptional events.

**Key words:** pentatricopeptide repeat protein, chloroplast gene expression, RNA binding protein, RNA maturation, RNA stabilization, RIP-chip

Jalal A., Schwarz C., Schmitz-Linneweber C., Vallon O., Nickelsen J., and Bohne A.-V. (2015). A Small Multifunctional Pentatricopeptide Repeat Protein in the Chloroplast of *Chlamydomonas reinhardtii*. *Mol. Plant* 8, 412–426.

## INTRODUCTION

Maintenance and regulation of chloroplast gene expression and biogenesis is mainly guaranteed by nucleus-encoded proteins that are specifically targeted to the organelle. Many of these factors belong to a class of RNA binding proteins, the pentatricopeptide repeat proteins (PPRs), which have been shown to participate in all stages of organellar gene expression (reviewed in, e.g., Barkan, 2011; Shikanai and Fujii, 2013; Barkan and Small, 2014).

PPRs are characterized by 2–30 tandemly arranged ~35-amino-acid repeats, each of which is predicted to form a pair of short  $\alpha$  helices (reviewed in Schmitz-Linneweber and Small, 2008). The repeat motifs themselves are only weakly conserved and

are assumed to mediate the sequence-specific binding of single-stranded RNA ligands by a modular mechanism (Barkan et al., 2012; Yagi et al., 2013). Based on *in silico* and *in vitro* analysis of PPR proteins and their respective target sequences, it has been proposed that a certain combination of amino acids of each PPR motif recognizes one specific nucleotide of the target RNA (Fujii et al., 2011; Barkan et al., 2012; Fujii et al., 2013; Takenaka et al., 2013; Yagi et al., 2013; Hammani et al., 2014). The first crystal structures of PPR proteins have appeared only recently, and their analysis supports the idea that specific amino acids at certain positions within the PPR

## A Multifunctional Algal PPR Protein

helices mediate the binding to distinct nucleotides in the interacting RNAs (Ban et al., 2013; Yin et al., 2013).

The binding of PPR proteins to their target sequences, which are often located in 5' or 3' untranslated regions (UTRs), introns, or intergenic regions of polycistronic mRNAs, can determine the stability, processing, editing, and/or translation of the transcript (Stern et al., 2010; Hammani et al., 2014). It is generally assumed that the binding site of a PPR protein within UTRs or intergenic regions of its target RNA defines the RNA termini by blocking exoribonucleases (reviewed in Barkan, 2011). However, their precise mode of action has been described only in a few cases (e.g. Nakamura et al., 2003; Kobayashi et al., 2012; Zhelyazkova et al., 2012). One outstanding example is the detailed analysis of the chloroplast protein PPR10 from maize, which binds to a 17-nt sequence in the *atpI-atpH* intergenic region, blocking both 5' → 3' and 3' → 5' exoribonucleases, thereby stabilizing both *atpI* and *atpH* transcripts. Furthermore, PPR10 appears to enhance the translation of the *atpH* transcript by remodeling the conformation of its ribosome binding site (Pfalz et al., 2009; Prikryl et al., 2011).

The PPR gene family is universally distributed in eukaryotes, with only few members occurring in non-plant organisms like mammals and fungi, while several hundred are found in terrestrial plants (reviewed in Lightowlers and Chrzanowska-Lightowlers, 2008; Fujii and Small, 2011; Lipinski et al., 2011; Hammani et al., 2014). The large numbers of PPRs in land plants (e.g. 450 in *Arabidopsis*; 477 in rice), where they represent one of the largest known protein families, stands in marked contrast to the limited numbers of PPRs encoded by the genomes of green algae. Thus, a recent comprehensive *in silico* analysis of algal PPRs identified only 14 proteins in the unicellular green alga *Chlamydomonas reinhardtii*, with the best-endowed species being *Chlorella* sp. N64A with 25 genes (Tourasse et al., 2013).

While PPRs have been intensively analyzed in higher plants for more than a decade, little is known about their counterparts in less complex photosynthetic eukaryotes. So far, only two algal PPRs, the *C. reinhardtii* proteins MCA1 and MRL1, have been functionally characterized. MCA1 stabilizes the *petA* mRNA that encodes cytochrome *f* and enhances its translation by binding to its 5' UTR (Raynaud et al., 2007; Loiselay et al., 2008; Boulouis et al., 2011). MRL1, on the other hand, is involved in the stabilization of *rbcL* mRNA, which codes for the large subunit of Rubisco (Johnson et al., 2010).

As the molecular analysis of this small set of algal PPRs is particularly interesting from an evolutionary point of view, we decided to investigate the function of another, unusually small PPR protein from *C. reinhardtii*, PPR7.

## RESULTS

### PPR7, a Small PPR Protein in *C. reinhardtii*

PPR7 (Cre01.g048750) is one of the two unusually small PPRs in *C. reinhardtii* (Tourasse et al., 2013). In contrast to most other algal PPRs, the protein is conserved across the entire Chlorophyta (Supplemental Figure 1). Sequencing of the EST clone LCO31f03-r (GenBank Accession No. AV621129) from the

Kazusa DNA Research Institute confirmed the predicted coding sequence of the gene model (chromosome\_1:6771579.6774128, on the minus strand) available on Phytozome (<http://www.phytozome.net>), while the sizes of the UTRs were slightly different from those proposed. The 1344-nt PPR7 transcript contains four exons, comprising a 666-nt coding sequence flanked by untranslated regions of 163 and 515 nt at its 5' and 3' ends, respectively. The predicted protein has 221 amino acids with a molecular mass of 24.3 kDa. *In silico* analysis of the N-terminal region of PPR7 with Predalgo (<https://giavap-genomes.ibpc.fr/predalگو>; Tardif et al., 2012) indicated a chloroplast localization, while TargetP (<http://www.cbs.dtu.dk/services/TargetP>; Emanuelsson et al., 2000) and Predotar (<http://urgi.versailles.inra.fr/predotar/predotar.html>; Small et al., 2004) suggested mitochondrial targeting. The transit peptide predicted by ChloroP (<http://www.cbs.dtu.dk/services/ChloroP>; Emanuelsson et al., 1999) is 41 residues long, yielding a deduced molecular weight of 19.9 kDa for the mature protein.

In contrast to most plant PPR proteins identified so far, which contain ~12 PPR repeats on average (Lurin et al., 2004; Tourasse et al., 2013), PPR7 consists of only four PPR units, followed by a very short, positively charged conserved tail (Supplemental Figure 1). Based on the secondary and 3D structure predictions, each of these repeats forms a pair of  $\alpha$  helices, as described for other PPR motifs (Supplemental Figure 2). Analysis of two quantitative RNAseq studies that compared the gene expression patterns of *Chlamydomonas* cells cultured under phototrophic (CO<sub>2</sub>) and mixotrophic (acetate) growth conditions showed that, in both studies and both conditions, PPR7 is the most highly expressed of all PPR genes, at least at the mRNA level (Castruita et al., 2011; Urzica et al., 2012; Supplemental Table 1).

### PPR7 Is Localized in the Chloroplast Stroma

To confirm the predicted organellar localization of PPR7, a PPR7-GFP fusion protein was expressed in *C. reinhardtii*. As shown in Figure 1A, the PPR7-GFP signal co-localized with the chlorophyll autofluorescence of the single cup-shaped chloroplast. Moreover, no co-localization of the PPR7-GFP signal and the MitoTracker-labeled mitochondria was observed, indicating that PPR7 is targeted solely to the chloroplast.

To substantiate this finding, immunoblot analyses were performed on subfractions of wild-type (WT) cells. Using a polyclonal antiserum raised against recombinant PPR7 protein, we detected a polypeptide with the expected molecular weight of ~20 kDa in total cell extracts and in the chloroplast fraction (Figure 1B). Moreover, like the stromal heat-shock protein HSP70B, PPR7 was considerably enriched in the soluble stromal compartment, and was undetectable in the crude thylakoid membrane and mitochondrial fractions. Therefore, PPR7 appears to be a soluble protein that resides in the chloroplast stroma.

### PPR7 Is a Component of a High-Molecular-Weight, RNase-Sensitive Complex

Most PPR proteins are found in RNase-sensitive, high-molecular-weight (HMW) complexes (e.g. Fisk et al., 1999; Meierhoff et al., 2003; Schmitz-Linneweber et al., 2006; Gillman et al., 2007; Johnson et al., 2010). To ascertain whether PPR7 forms part of

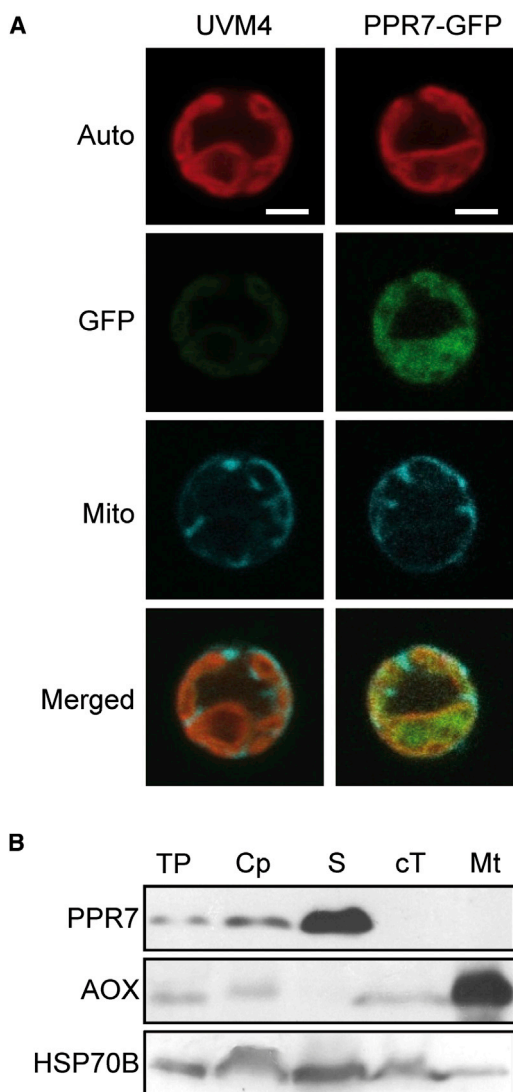


**Figure 1. PPR7 Is Localized to Chloroplast Stroma.**

**(A)** Green fluorescent protein (GFP) import assay. Expression pattern of GFP fused to the predicted transit peptide of PPR7 (PPR7-GFP) after stable transformation of the UVM4 strain. The untransformed recipient strain (UVM4) served as control. Cells were analyzed by laser scanning confocal microscopy. The panel shows chlorophyll autofluorescence (Auto), GFP fluorescence (GFP), the MitoTracker signal (Mito), and an overlay of all three (Merged). Bars represent 1 mm.

**(B)** Immunodetection of PPR7 in cell subfractions. Aliquots (50  $\mu$ g) of total proteins (TP), chloroplast (Cp), stroma (S), crude thylakoids (cT), and mitochondrial proteins (Mt) from wild-type cells, prepared as described in the Methods section, were analyzed using the antibodies indicated to the left of each panel. The alternative oxidase (AOX) and the heat-shock protein 70B (HSP70B) served as markers for mitochondria and stroma, respectively.

a ribonucleoprotein (RNP) complex, size-exclusion chromatography (SEC) of chloroplast stroma was performed, with and without prior treatment of samples with RNase. By following the elution pattern of PPR7, we found that it forms a part of an HMW complex that elutes in the size range between 440 and 1000 kDa (Figure 2, upper panel, fractions 2–9). The main peak of PPR7 was observed in fractions 4–7, which correspond

## A Multifunctional Algal PPR Protein

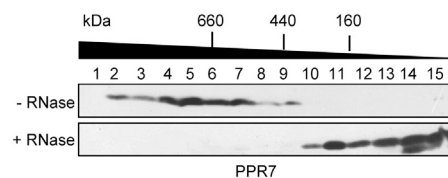


**Figure 2. PPR7 Is a Component of a High-Molecular-Weight Ribonucleoprotein Complex.**

Stromal proteins (~2 mg) from the wild-type strain CC406 were fractionated by size-exclusion chromatography in the absence (–RNase) or presence (+RNase) of 250 U RNase One. Fractions 1–15 were subjected to immunoblot analysis using a PPR7-specific antiserum. Molecular weights were calculated by parallel analysis of HMW calibration markers. Elution profiles of marker proteins (kDa) are shown at the top, together with the respective fraction numbers.

to a complex size of 500–800 kDa. In the presence of RNase, however, the complex size was dramatically reduced to  $\leq$ 300 kDa (Figure 2, lower panel, fractions 10–15). These findings thus demonstrate that PPR7 indeed forms part of an RNP complex.

Moreover, as PPR7 has a molecular weight of only ~20 kDa, the size of the RNase-resistant complexes implies that it must associate with other proteins (and/or with itself as an oligomer) even in the absence of RNA. Taken together, these data show that PPR7 is a component of an HMW complex that interacts with RNA *in vivo*.

## PPR7 Is Associated with Multiple Chloroplast Transcripts

To identify the RNA ligands of PPR7, the protein was immunoprecipitated from chloroplast stroma, and co-precipitated RNAs were subjected to a microarray-based chip hybridization, a method that is well established for higher plants but has not previously been applied to green algae (RIP-chip; Schmitz-Linneweber et al., 2005). As confirmed by immunoblot analysis, the PPR7 protein could be quantitatively precipitated from WT stroma, whereas it was not detected in the precipitate obtained with pre-immune serum (Figure 3A).

In parallel, RNAs were purified from the pellet and supernatant of each immunoprecipitation and used to probe a microarray consisting of 166 overlapping PCR products representing the complete *C. reinhardtii* chloroplast genome, and 15 overlapping PCR products representing the complete mitochondrial genome. Intriguingly, comparison of the RIP-chip signal intensities obtained for the RNAs precipitated by PPR7 antiserum and pre-immune serum indicated that, relative to other PPR proteins, PPR7 recognizes an unusually large number of RNAs as binding partners. Top RNA enrichment peaks were found for protein-encoding genes/gene clusters *psbH-trnE2*, *rpoC2*, *rbcL/atpA*, *cemA-atpH*, *atpl-psaJ*, as well as DNA sequences corresponding to the non-coding *16S* and *tscA* RNAs in the chloroplast genome (Figure 3B and Supplemental Table 2).

The RIP-chip data were validated by semi-quantitative RT-PCR of RNAs purified from pellet and supernatant fractions of immunoprecipitations performed with pre-immune and anti-PPR7 sera as described above. cDNAs were amplified using primers

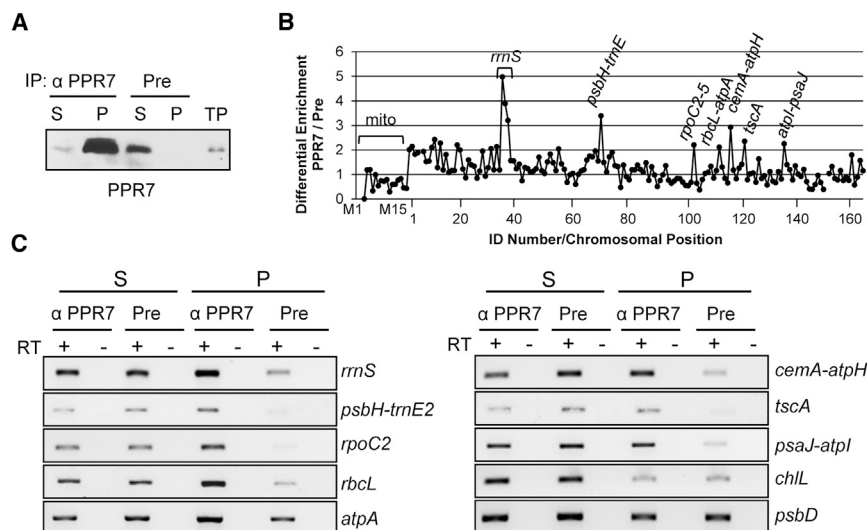


**Figure 3. Association of PPR7 with Chloroplast Transcripts.**

against PPR7 and four control assays using pre-immune serum. The median normalized values for replicate spots from the PPR7 immunoprecipitations were divided by those from pre-immune controls, and are plotted according to fragment number on the *C. reinhardtii* organellar genome microarray. Fragments are numbered according to chromosomal position (the first 15 fragments represent mitochondrial genes). Gaps in the graph indicate PCR products that did not meet quality standards as defined in Schmitz-Linneweber et al. (2005). The data used to generate this figure are provided in Supplemental Table 2. PCR product identity numbers for putative PPR7 targets according to Supplemental Table 3 are as follows: *rrnS* (IDs 35–37), *psbH-trnE2* (ID 70), *rpoC2* (ID 103), *rbcL/atpA* (ID 112), *cemA-atpH* (ID 116), *tscA* (ID 122), and *psaJ-atpI* (ID 136).

(C) RT-PCR analysis of RNA that co-purified with PPR7. RT-PCR was performed using primer sets specific for the genes indicated to the right of each panel. RNA used for RT-PCR was obtained from co-immunoprecipitation of PPR7 supernatant (S) and precipitate (P), using a PPR7-specific antibody ( $\alpha$  PPR7) as described in Methods. Pre-immune serum (Pre) was used as a control. RT+ indicates the presence and RT- the absence of reverse transcriptase in the RT reaction to exclude amplification of contaminating DNA fragments. *chlL* and *psbD* were used as controls. PCR products were subjected to DNA electrophoresis. The results shown are representative of three independent RT-PCRs carried out with each primer set.

specific for all putative PPR7 targets, as well as the two control genes *chlL* and *psbD*, which are assumed not to represent PPR7 targets based on the RIP-chip analysis (see also Supplemental Table 2). As shown in Figure 3C, all PCR products resulting from amplification of potential target sequences from the PPR7 precipitate were clearly more abundant than those amplified from pre-immune precipitates, whereas PCR products amplified from precipitates of both control gene sequences were equally represented. Hence, all seven putative target RNAs were validated by this independent approach, thereby confirming the binding of PPR7 to these transcripts.

### PPR7 Is a Multifunctional Protein Required for Chloroplast Gene Expression

The heterogeneous nature (various mRNAs as well as non-coding RNAs such as *tscA* and 16S rRNA) and the unusually high number of RNA targets identified in RIP-chip analysis suggests that PPR7 has diverse functions in RNA metabolism. Unfortunately, attempts to demonstrate an RNA binding activity of PPR7 *in vitro* using two different versions of recombinant PPR7 consisting of amino acids 44–221 (rPPR7-1) or 61–221 (rPPR7-2), respectively, remained inconclusive. The binding activity detected was very low, although this may be related to the protein's tendency to precipitate under the conditions employed (data not shown). Considering that the protein is predicted to consist mainly of  $\alpha$ -helical repeat regions, incorrect folding of rPPR7 was also indicated by the low content of  $\alpha$ -helical structure (23% for rPPR7-1 or ~30% for rPPR7-2) revealed by circular dichroism spectroscopy (Supplemental Figure 3).

To elucidate PPR7's role in chloroplast gene expression, PPR7 RNAi strains were generated. Depletion of PPR7 accumulation was most effective in three transformants, named *iPPR7*-1, -2, and -3 (Figure 4A), which exhibited residual protein levels equivalent to ~15%, ~30%, and ~35% of that in the recipient strain transformed with the empty vector (hereafter called WT).

### Reduction of PPR7 Levels Leads to Photosensitivity

To investigate the effect of PPR7 knockdown in these *iPPR7* strains, growth tests were performed on agar plates (Figure 4B). The PPR7-depleted strains showed no significant growth defect under mixotrophic growth conditions in moderate light (ML) or under heterotrophic conditions in the dark (D), but their growth rates were clearly diminished under photoautotrophic conditions, suggesting a reduced ability to perform photosynthesis. In accordance with the relative impact of RNAi on the accumulation of PPR7, the strongest growth retardation was observed for strain *iPPR7*-1. This strain also exhibited a photosensitive phenotype, as its growth rate under mixotrophic conditions in higher light (HL) was extremely low. However, strong growth retardation was not observed when cells were grown in liquid cultures under mixotrophic or photoautotrophic conditions in HL (Figure 4D). We therefore assume that the pronounced light-sensitive phenotype on plates is due to the absorption of HL energy by cells on plates as compared with liquid cultures.

Liquid cultures grown mixotrophically in ML showed no evidence for a photosystem II (PSII) or RbcL deficiency, as judged from fluorescence induction kinetics. Fv/Fm was 0.80 for *iPPR7*-1 and *iPPR7*-3 and 0.78 for *iPPR7*-2, versus 0.80 for the WT control.

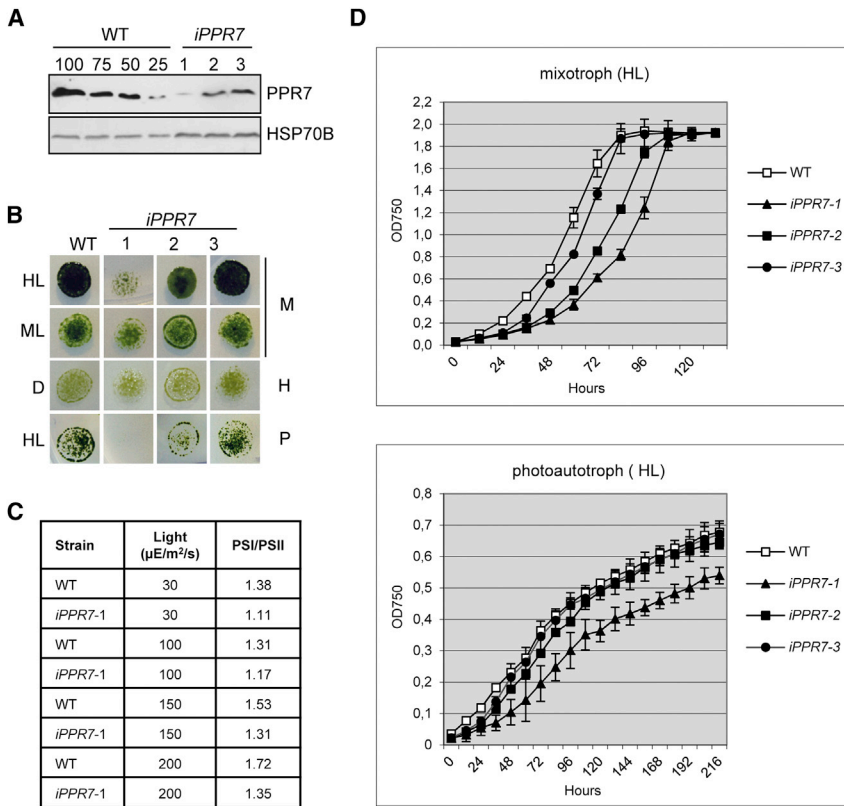


**Figure 4. Growth Phenotype of *iPPR7* Strains and Accumulation of Chloroplast Proteins.**

**(A)** PPR7 protein accumulation. Immunoblot analysis of total soluble proteins (100  $\mu\text{g}$ ) isolated from the indicated *iPPR7* strains 1–3 and the wild-type (WT) (a dilution series of the WT sample from 100% to 25% was applied to the gel) was performed with PPR7-specific antiserum. HSP70B served as loading control for stromal proteins.

**(B)** Phenotypic characterization of *iPPR7* strains under different growth conditions. Drop tests were performed by spotting 20- $\mu\text{l}$  aliquots of cultures resuspended in High Salt Minimal (HSM) medium at a density of approximately  $1 \times 10^6$  cells/ml. The three indicated *iPPR7* mutants (1–3), together with the WT, were grown under mixotrophic (M), photoautotrophic (P), or heterotrophic (H) conditions under higher light (HL), moderate light (ML), or in the dark (D).

**(C)** Electrochromic shift (ECS) measurements. PSI/PSII ratios were measured using ECS in cultures grown mixotrophically at 30 or 200  $\mu\text{E}/\text{m}^2/\text{s}$ , as well as in cells transferred for 4 h from 30 to 100 or 150  $\mu\text{E}/\text{m}^2/\text{s}$ .

**(D)** Growth curves of *iPPR7* strains. Growth rates were determined under mixotrophic (upper panel) or photoautotrophic (lower panel) growth conditions at 100  $\mu\text{E}/\text{m}^2/\text{s}$  by measuring OD<sub>750</sub>. Error bars represent standard deviation (SD) from the mean based on results from three independent cultures.

Electrochromic shift (ECS) measurements performed for *iPPR7-1* indicated a reduced photosystem I (PSI)/PSII ratio compared with the control, which might be caused by a slight PSI deficiency. This was observed in ML as well as in HL, or when ML-grown cells were transferred to 100 or 150  $\mu\text{E}/\text{m}^2/\text{s}$  (Figure 4C). In HL intensities, PSII activity declined similarly in control and *iPPR7* strains, leading to a similar increase in PSI/PSII activity ratios.

Light sensitivity has often been described for photosynthesis-defective mutants, in particular for mutants in PSI, ATPase, or Rubisco (e.g. Spreitzer and Mets, 1981; Majeran et al., 2001; Sommer et al., 2003; Johnson, 2011). We therefore measured the steady-state levels of subunits of the major chloroplast protein complexes in *iPPR7* strains. As shown in Figure 5, the relative lack of PPR7 in the three analyzed RNAi strains grown under moderate or higher light conditions had no significant impact on the accumulation of the ATP synthase  $\beta$  subunit (AtpB), the large subunit of Rubisco (RbcL), the D2 reaction center protein of PSII (D2), or a subunit of the cytochrome *b<sub>6</sub>f* complex (Cytb6). These are central subunits of their respective protein complexes and cannot accumulate in the absence of their assembly partners (Choquet et al., 2001; Drapier et al., 2007). Hence, we can conclude that the ATP synthase, Rubisco, PSII, and cytochrome *b<sub>6</sub>f* complexes accumulate to WT levels in the PPR7 RNAi strains. However, independently of the growth conditions tested, the PSI reaction center protein PsaA was clearly reduced in all three knockdown strains compared with the WT recipient strain. PsaA levels were reduced to  $\sim 35\%$  of WT in *iPPR7-1*,  $\sim 40\%$  *iPPR7-2*, and  $\sim 60\%$  in *iPPR7-3*, which more or less correlates with the

amount of residual PPR7 protein in these strains. The resulting PSI deficiency could be responsible for their photosensitive phenotype, as PSI mutants are known to be exquisitely light sensitive (e.g. Spreitzer and Mets, 1981).

### PPR7 Is Involved in the Stabilization of Chloroplast mRNAs

To better understand PPR7's role in chloroplast gene expression, we set out to elucidate its function in the expression of each of the target RNAs identified in the RIP-chip approach. To do so, we used RNA gel-blot analysis to assess the levels of precursors and mature transcripts of *rmS*, *psbH-tmE2*, *rpcO2*, *rbcL*, *atpA*, *cemA-atpH*, *tscA*, and *psaJ-atpI* in the three PPR7-deficient RNAi strains. As at least strains *iPPR7-1* and *iPPR7-2* showed a slight growth phenotype in liquid cultures when grown mixotrophically under HL we chose these conditions for the RNA analysis. However, to exclude secondary effects caused only by HL intensities, we exemplarily analyzed the accumulation of selected transcripts also under ML conditions (see below; Supplemental Figure 4). In addition, we investigated the accumulation of three chloroplast transcripts (*psbA*, *psbD*, and *psbB*), which are not targets of PPR7 based on the RIP-chip analysis.

The analysis of the non-target mRNAs *psbA*, *psbD*, and *psbB* revealed no altered accumulation in *iPPR7* strains in comparison with the WT. Therefore, a general defect in RNA accumulation in these strains is unlikely (Supplemental Figure 5). However, considering the high number of identified PPR7 target RNAs and the slight growth retardation of *iPPR7* strains in HL, we

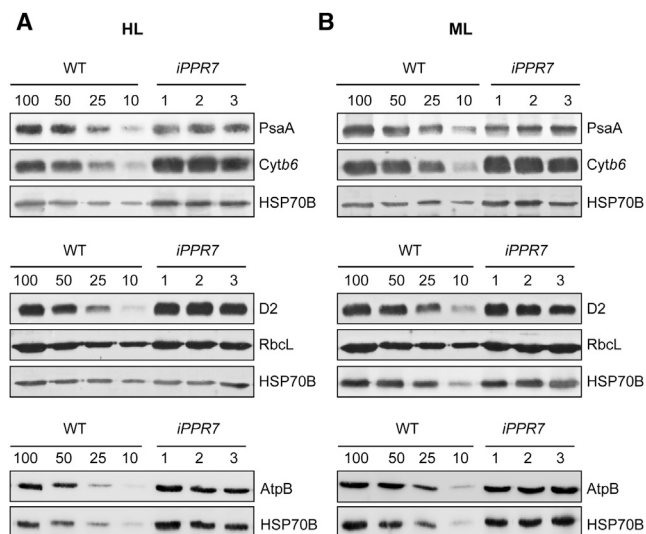


**Figure 5. Immunoblot Analysis of Representative Photosynthesis-Related Protein Complexes in *iPPR7* Strains.**

Total proteins (30  $\mu$ g) from *iPPR7* strains 1–3 and wild-type (WT) cells grown mixotrophically under higher (A) or moderate (B) light conditions were probed with antibodies against individual subunits of PSI (PsaA), the *Cytb6/f* complex (*Cytb6*), PSII (D2), Rubisco (RbcL), and the  $\beta$  subunit of chloroplast ATP synthase (AtpB). HSP70B served as a loading control.

cannot completely exclude minor secondary effects on other chloroplast RNAs in these strains. One putative PPR7 binding site was identified within a region that spans the 5' ends of the *rbcL* gene and the *atpA* gene cluster, which are disposed in opposite orientations on the chloroplast genome (Figure 6A, top panel). To investigate the steady-state levels of *rbcL* transcripts, we used a probe that detects the major 1.5-knt mRNA, as well as a minor transcript of 2.9 knt, whose precise 5' and 3' ends are not known (Figure 6A). Compared with the WT, the intensity of the 2.9-knt band was much decreased (to  $\sim$ 40% of WT) in all *iPPR7* strains, suggesting that it is less stable in these strains. However, the mature *rbcL* mRNA was only slightly affected in the knockdown strains, with  $\sim$ 85% of the WT level remaining in the most depleted RNAi strain *iPPR7-1* (Figure 6A).

Next we investigated *rpoC2* transcripts that code for the  $\beta'$  subunit of the plastid-encoded RNA polymerase PEP. Here, the putative PPR7 binding site was identified in the central part of the coding region (Figure 6B, upper panel). As shown in Figure 6B (middle and bottom panels), RNA blot analysis revealed a low-abundance transcript of  $\sim$ 9 knt, which corresponds to the size of the *rpoC2* gene in the chloroplast genome. This mRNA was reduced in all three *iPPR7* strains to  $\sim$ 75%–85% of the WT level, suggesting a stabilizing effect of the PPR7 protein on *rpoC2* transcripts also. A comparable reduction of this transcript was also observed when strains were grown under ML conditions, which indicates that the reduced transcript accumulation is not caused by secondary effects in HL (Supplemental Figure 4A).

A further putative binding site for PPR7 was identified in a region covering the *psbH* gene and the downstream *trnE2* gene. However, no hit was obtained for the downstream PCR product in the RIP-chip analysis, which encompasses the complete *trnE2* gene as well as 85 bp upstream of the mature tRNA (ID 69,

Supplemental Table 2), suggesting that *trnE2* is not a target of PPR7. The *psbH* gene is part of the *psbB-psbT-psbH* gene cluster and codes for a small thylakoid membrane protein (PsbH) that is associated with light-dependent control of PSII activity in *C. reinhardtii* (Johnson and Schmidt, 1993; O'Connor et al., 1998). On the RNA gel blot (Figure 6C, top panel), a probe covering the coding region of *psbH* gene detected transcripts with sizes of 0.9, 0.8, 0.5, and 0.4 knt (Figure 6C, top and middle panels), which have previously been reported to share the same 5' end and differ in the lengths of their 3' UTRs (Johnson and Schmidt, 1993). All four transcripts were slightly but reproducibly reduced in the three *iPPR7* strains in comparison with the WT, with the most pronounced effect again being observed in strain *iPPR7-1* (Figure 6C, middle and bottom panels). As the upstream PCR product covering the *psbH* 5' UTR gave no comparable signal in the RIP-chip analysis, we assume that stabilization of the monocistronic *psbH* transcript is mediated via PPR7's association with the *psbH* CDS or its immediately adjacent 3' region.

Taken together, these effects on steady-state levels of the long *rbcL* transcript, the *rpoC2* transcript, and the monocistronic *psbH* transcripts in PPR7-depleted strains suggest that PPR7 contributes, albeit marginally, to the stabilization or production of these transcripts.

### PPR7 Is Involved in the Processing of Chloroplast mRNAs

Another potential PPR7 binding site was identified in association with the *atpI* and *psaJ* intergenic region in the *psbJ-atpI-psaJ-rps12* gene cluster (Figure 7A, upper panel). The proteins encoded by these co-transcribed genes are PsbJ, a PSII reaction center protein, subunit IV of the ATPase, the PSI reaction center subunit PsaJ, and the ribosomal protein S12, respectively.

To investigate the role of PPR7 in the expression of this polycistronic transcript, RNA gel-blot analysis was performed using a probe covering the 3' region of the *atpI* coding sequence, the intergenic region of *atpI-psaJ*, and the coding region of *psaJ*. We observed a complex transcript pattern, as has been reported before (Figure 7A; Liu et al., 1989; Rymarquis et al., 2006). Unfortunately, the precise identity of all of the detected transcripts has not yet been defined. However, we did detect a slightly increased accumulation of the 2.9-knt tetracistronic species (transcript a in Figure 7A) in the RNAi strains relative to the WT, and a decrease in levels of the processed transcripts (b, c, d), with the most pronounced effect being seen in strains *iPPR7-1* and *iPPR7-2*. This suggests a potential function of PPR7 in the maturation of *psbJ-atpI-psaJ-rps12* transcripts. Furthermore, the reduction of mature *psaJ* mRNA may contribute to the observed light sensitivity of *iPPR7-1* and *iPPR7-2* stated above. According to Fischer et al. (1999), a deletion of the *psaJ* gene leads to reduced PSI efficiency caused by the compromised capability of PSI to oxidize Cytb6/plastocyanin.

The *atpA* gene cluster in the *C. reinhardtii* chloroplast genome consists of the genes *atpA*, *psbI*, *cemA*, and *atpH*, which code for the  $\alpha$  subunit of the ATP synthase, a small PSII subunit, a putative envelope membrane protein involved in inorganic carbon

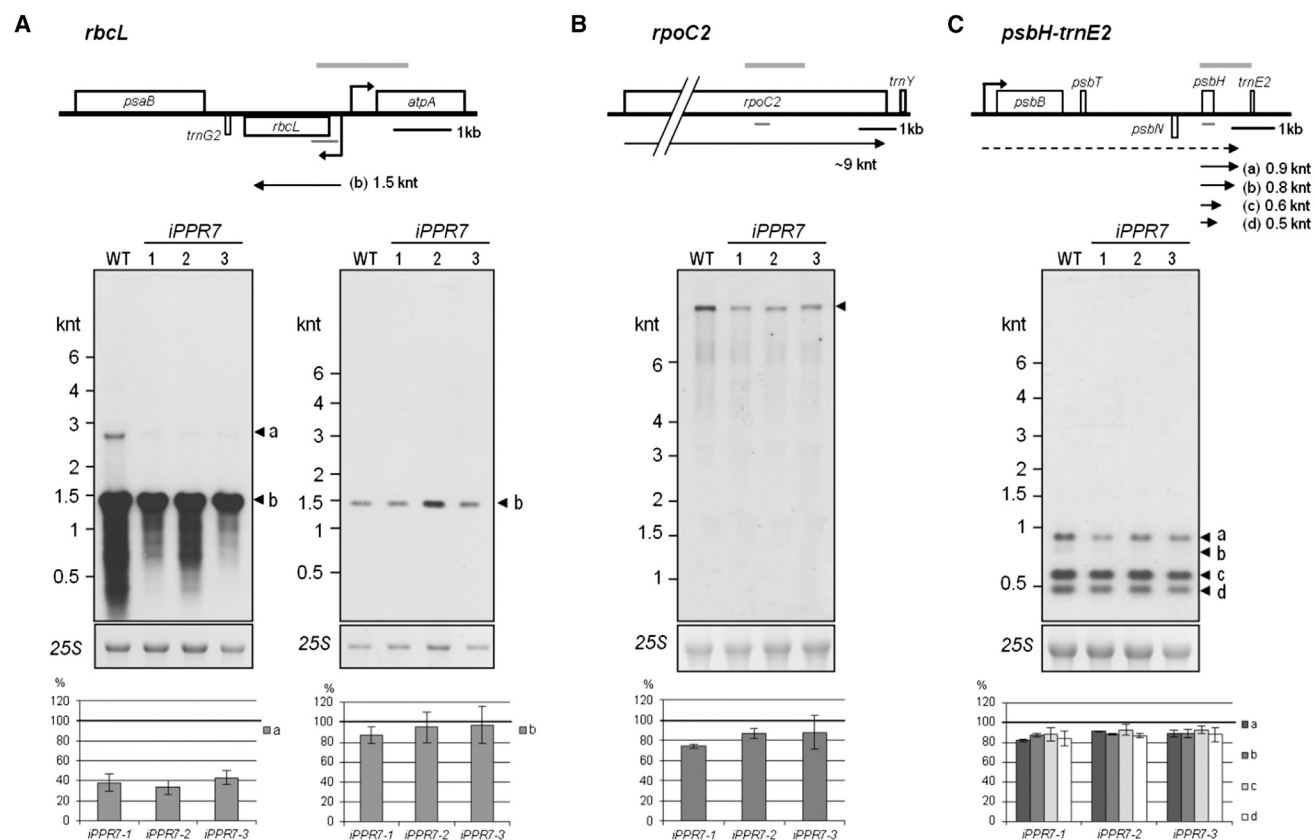


**Figure 6. PPR7 Is Involved in the Stabilization of Specific Chloroplast mRNAs.**

RNA gel-blot analysis of *rbcL* (A), *rpoC2* (B), and *psbH-trnE* (C) transcripts. Schematic diagrams of the respective genes in the chloroplast genome are shown in the upper panels. The open boxes represent the genes. Genes above the line are transcribed from left to right, genes below the line from right to left. The PPR7 binding fragments identified by RIP-chip analysis are indicated as gray boxes above the models. Positions of probes used for RNA blot analysis are indicated as gray bars below the models. Transcripts and their respective sizes according to Johnson and Schmidt (1993) for *psbH*, and according to Johnson et al. (2010) for *rbcL*, are indicated by black arrows. The identity of the 2.9-knt *rbcL* transcript (a) observed in this study is unknown and is therefore not depicted in the scheme. Mapped promoters for the *psbB* cluster (Monod et al., 1992) and the *rbcL* cluster (Salvador et al., 1993) are represented by bent arrows. Middle panels: For RNA blot analysis using the probes indicated in the corresponding upper panels, 10- $\mu$ g aliquots of total cellular RNA extracted from WT and *iPPR7* strains 1–3 grown mixotrophically at HL were used for the detection of *psbH* and *rpoC2* transcripts. For the detection of the *rbcL* precursor (A, left panel) and mature *rbcL* transcripts (A, right panel) 5  $\mu$ g or 200 ng of RNA were used, respectively, to obtain quantifiable signals from the highly abundant mature *rbcL* transcript. The ethidium bromide-stained gels displaying the 25S rRNAs are shown as loading controls (25S). The positions of RNA size markers (sizes are given in kilonucleotides) are indicated to the left of each blot. Lower panels: Quantification of signal intensities. The hybridization signals were normalized to the respective signals for 25S rRNA and the WT signal was set to 100%. Error bars represent SDs from three independent experiments.

uptake, and subunit III of the chloroplast ATP synthase, respectively (Drapier et al., 1998; Figure 7B, upper panel). The RIP-chip analysis detected two hits within this gene cluster: the first overlaps the 5' region of *atpA* (see above) and the second covers the 3' region of *cemA* and the entire coding region of *atpH* (Figure 7B, upper panel). For transcript analysis we designed two probes. Probe P1 was derived from the 5' UTR of *atpA* and detected the monocistronic *atpA*, the dicistronic *atpA-psbI*, the tricistronic *atpA-psbI-cemA*, and the tetracistronic *atpA-psbI-cemA-atpH* transcripts (Figure 7B, left panels), whereas probe P2 extended from the 3' end of *cemA* to the 3' end of *atpH* and detected the unprocessed tetracistronic RNA, as well as the tricistronic *psbI-cemA-atpH* and monocistronic *atpH* transcripts (Figure 7B, right panels).

Whereas mutants *iPPR7-2* and *iPPR7-3* revealed only negligible alterations in the accumulation of all the transcripts analyzed,

we observed that the tricistronic (4.6 knt) and tetracistronic (5.3 knt) species were present in higher abundance (~130%–140% compared with the WT) in *iPPR7-1*, the strain most effectively depleted of PPR7. This result, together with the presence of two putative PPR7 binding sites within the tetracistronic RNA, suggests that PPR7 is also involved in the processing of the polycistronic *atpA* transcripts. Note that, even though the precursors over-accumulated in *iPPR7-1*, we observed at most a slight reduction in levels of the much more abundant, processed monocistronic and dicistronic transcripts. This indicates that PPR7 depletion impairs processing only partially and does not destabilize the mature transcripts.

#### PPR7 Is Involved in Processing of Chloroplast 16S rRNA and Accumulation of the Non-Coding *tscA* RNA

Several signals obtained in the RIP-chip analysis suggested the presence of putative PPR7 binding sites in non-coding RNAs.

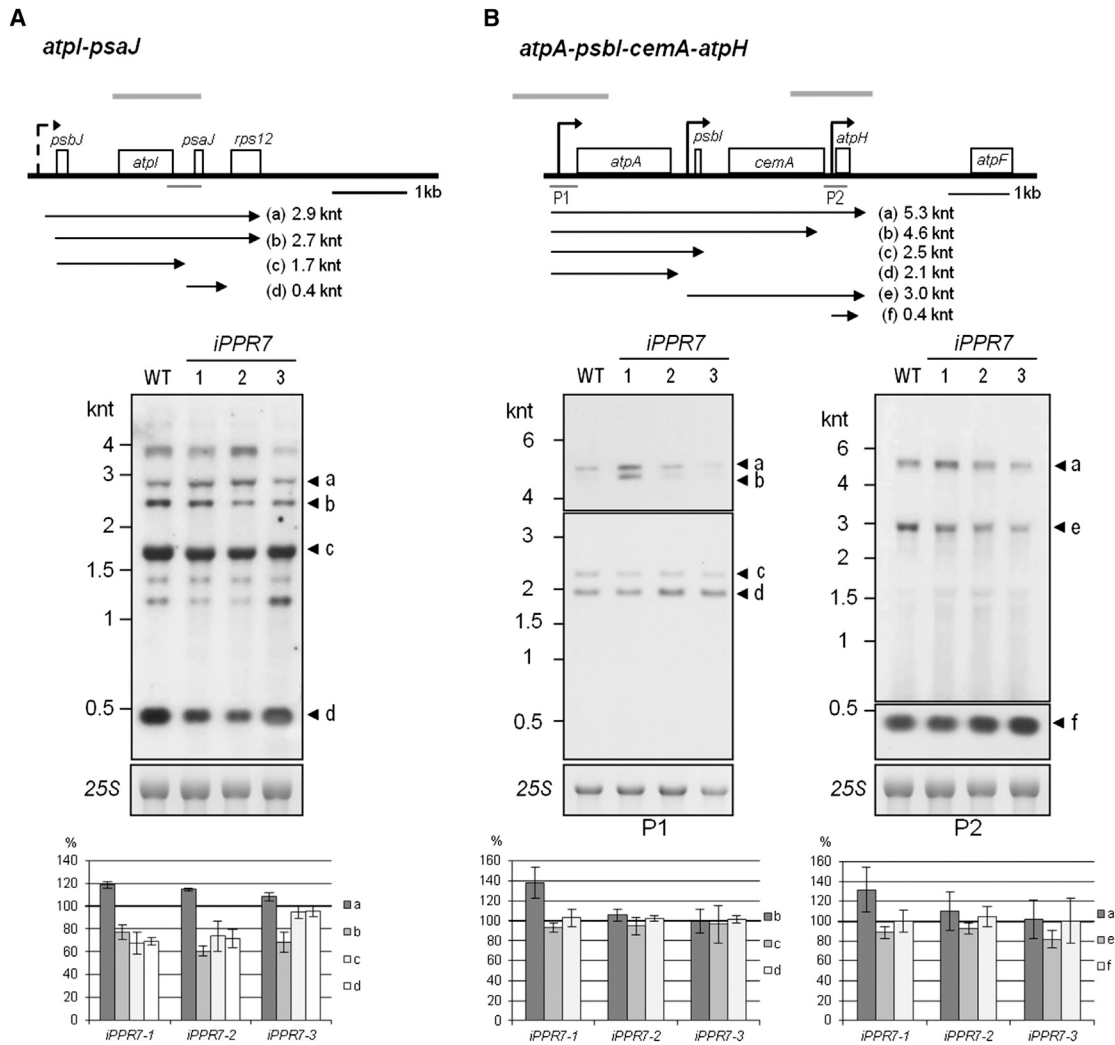


**Figure 7. PPR7 Is Involved in the Processing of Certain Chloroplast mRNAs.**

RNA blot analysis of *atpI-psaJ* (A) and *atpA-psbI-cemA-atpH* (B) transcripts of cells grown mixotrophically under higher light conditions. Labeling and quantification methods are described in Figure 6. Promoter position and respective sizes of transcripts for the *psaJ-atpI* cluster and the approximate position of the promoter upstream of *psbJ* are given according to Liu et al. (1989) and Rymarquis et al. (2006), respectively, and for the *atpA-psbI-cemA-atpH* cluster according to Drapier et al. (1998). For the hybridization shown in (A), 10- $\mu$ g aliquots of total cellular RNA were used; for the hybridization shown in (B), 2  $\mu$ g (left) and 10  $\mu$ g (right) of total cellular RNA was used. The upper portions of both blots are extended exposures of the same blots to visualize signals for the low-abundance polycistronic transcripts (a, b, and e).

As depicted in Figure 8A (upper panel), we obtained three consecutive hits in the *rrnS* region encoding the 16S ribosomal RNA (rRNA). The 16S rRNA gene is part of the *rrn* operon consisting of genes encoding 16S, 7S, 3S, 23S, and 5S rRNAs, as well as two tRNAs (*trnI* and *trnA*). To analyze the size, composition, and relative abundance of transcripts from this cluster in *iPPR7* strains, RNA gel-blot analysis was performed using three different probes as indicated in Figure 8A. The first probe, located upstream of the 5' end of *rrnS* (P1), labeled an HMW precursor transcript of  $\sim$ 7.3 knt (transcript a) corresponding to the entire stretch from 16S to 5S (Figure 8A, left panel). The relative abundance of this large precursor (transcript a) was found to be increased in all *iPPR7* strains, by  $\sim$ 70% compared with the WT level in *iPPR7-1*, and by  $\sim$ 20% in *iPPR7-2* and *iPPR7-3*. Conversely, the partially processed 16S transcript (transcript b) was underrepresented, attaining only

$\sim$ 70% of its level in WT. A similar transcript pattern using the same probe was detected also under ML conditions as described before for the *rpoC2* transcript (Supplemental Figure 4B). However, detection of the mature 16S rRNA (transcript c) with probe P2 revealed no obvious differences between *iPPR7* strains and the WT (Figure 8A, middle panel), which might be explained by the accumulation of the extremely stable 16S rRNA.

A third probe (P3) located in the intron region of the *rrnL* gene (23S) confirmed the increased abundance of the large precursor RNA (transcript a) seen with probe P1 in *iPPR7* strains (Figure 8A, right panels). In addition, probe P3 revealed reduced accumulation of the partially processed 3.8-knt transcript consisting of 7S, 3S, 23S, and 5S rRNAs (transcript d), as well as of the spliced intron sequence of 0.9 knt (transcript e), to  $\sim$ 80% or

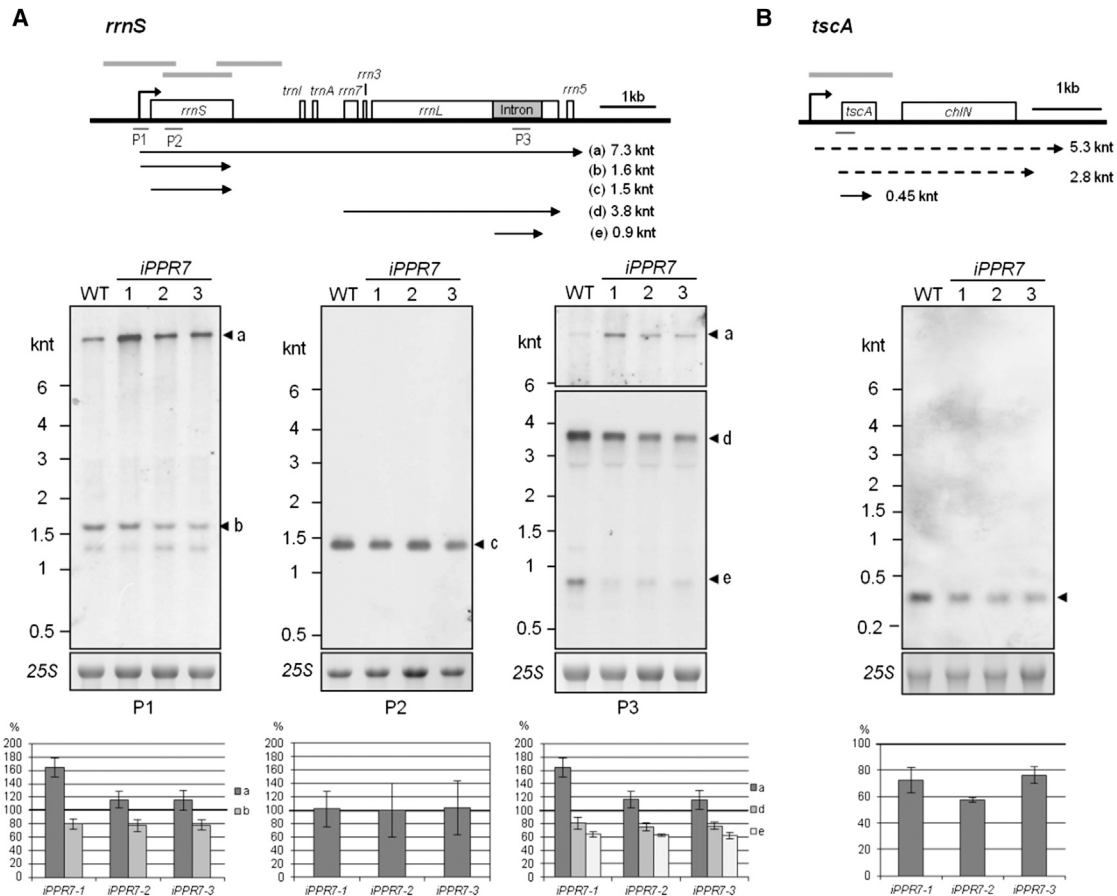


**Figure 8. PPR7 Is Involved in Processing of Chloroplast 16S rRNA and Accumulation of the Non-Coding *tscA* RNA.**

RNA blot analysis of the 16S rRNA (A) and the non-coding RNA *tscA* (B) of cells grown mixotrophically under higher light conditions. Labeling and quantification are described in Figure 6. Promoter position and respective sizes of transcripts for the *rrnS* cluster are given according to Holloway and Herrin (1998) and for *tscA* according to Goldschmidt-Clermont et al. (1991). Two low-abundance transcripts of 5.3 and 2.8 knt described by Hahn et al. (1998) representing *tscA-chlN* co-transcripts are indicated, but were not detectable under the conditions employed here. For the hybridization shown in (A), 10  $\mu$ g of RNA was used for blots probed with P1 and P3, while 1  $\mu$ g RNA was used for the blot probed with P2. The upper portion of the blot probed with P3 is an extended exposure to visualize the precursor transcript. For the detection of *tscA* RNA, 5  $\mu$ g of RNA was used.

60% of the WT level, respectively. Taken together, the data obtained for the *rrnS* gene cluster suggest a role of PPR7 in the maturation of the rRNA precursor transcript. Based on the RIP-chip analysis, the PPR7 binding site is proposed to lie in the 16S region, and the effect of PPR7 depletion on the maturation of the downstream 23S rRNA precursor is probably indirect and caused by disruption of the normal temporal sequence of processing events or defects in ribosome assembly. To investigate if this causes a general defect in protein synthesis,  $^{14}$ C-pulse labeling experiments were performed, which mainly detect highly synthesized PSII subunits (Supplemental Figure 6). None of these proteins was synthesized at lower rates in *iPPR7* strains compared with the WT, indicating that protein synthesis in PPR7-depleted strains is not generally affected.

The *psaA* gene of *C. reinhardtii* is composed of three exons located at different positions in the chloroplast genome, which are transcribed as separate precursors (reviewed in Rochaix, 1996). These precursors come together, and the two group II introns between exons 1 and 2 and exons 2 and 3 are trans-spliced to generate the mature *psaA* mRNA. Interestingly, intron

1 is formed by three components consisting of the precursors of exons 1 and 2, and the short non-coding RNA *tscA*, which is co-transcribed with *chlN* and then processed to yield a 450-nt mature form (Goldschmidt-Clermont et al., 1991). As part of the tripartite intron 1, *tscA* is necessary for trans-splicing of the *psaA* pre-transcript (reviewed in Jacobs et al., 2010). RIP-chip analysis identified the *tscA* RNA as a putative target of PPR7, and subsequent RNA gel-blot analysis revealed that the mature *tscA* transcript was reduced to ~60%–75% of the WT level in *iPPR7* strains (Figure 8B). No significant accumulation of the RNA precursors previously identified by Hahn et al. (1998) was observed under these growth conditions. Interestingly, these precursors accumulated to a higher extent in *iPPR7* strains compared with the WT when cells were grown mixotrophically in ML, while the mature *tscA* RNA displayed a reduction similar to that observed under HL (Supplemental Figure 4C), so that PPR7 appears to be involved in the stabilization and/or processing of the *tscA-chlN* transcript. As a reduction of *tscA* RNA might directly influence the formation of the trans-splicing intermediates, we further investigated the accumulation of *psaA* mRNAs using probes specific for exons 1, 2, and 3,

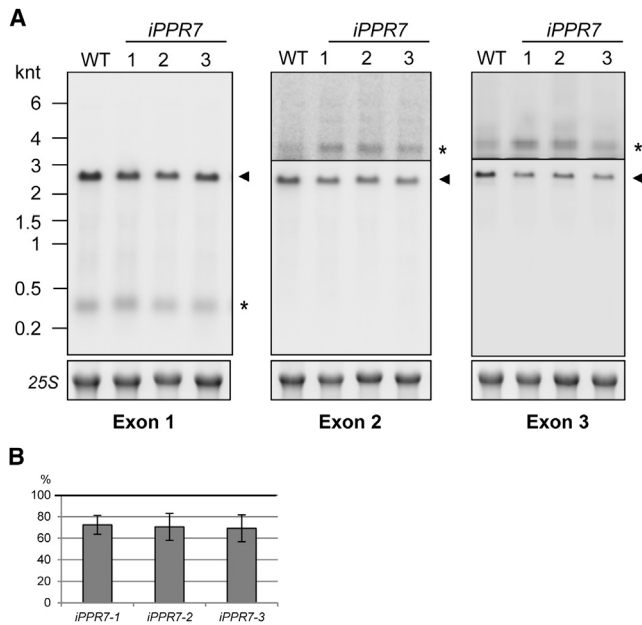


**Figure 9. Reduced Accumulation of *psaA* Transcripts.**

**(A)** RNA blot analysis of *psaA* transcripts from cells grown mixotrophically under higher light conditions. Used probes are specific for exon 1 (left panel), exon 2 (middle panel), and exon 3 (right panel), respectively. For hybridization, 5  $\mu$ g of total cellular RNA was loaded per lane. The upper portions of exon 2 and exon 3 blots are extended exposures of the same blots to visualize signals for the low-abundance precursor transcripts. The mature 2.8-knt *psaA* transcripts detected with all probes are labeled with arrowheads; distinct precursor transcripts are marked with asterisks. An overview of *psaA* trans-splicing events is depicted, for example, in Glanz et al. (2012).

**(B)** Quantitation of mature 2.8-knt *psaA* transcripts in *iPPR7* strains shown in **(A)**. Labeling and quantification are as described in Figure 6.

respectively (Figure 9). All probes revealed a decrease in accumulation of the mature 2.8-knt *psaA* transcripts in *iPPR7* strains, down to  $\sim$ 70% of the WT level, while processing intermediates appeared slightly increased. This suggests an indirect role for PPR7 in the accumulation of *psaA* transcripts, via its effect on *tscA*, and is compatible with the observed decrease in levels of the PsaA protein in *iPPR7* strains (see Figure 5).

## DISCUSSION

In this study, we analyzed the molecular function of the small PPR7 protein from *C. reinhardtii*. PPR7 resides in the chloroplast stroma, and is a component of an HMW RNase-sensitive complex. Unlike other PPR proteins, which generally appear to target one or very few RNA species, RIP-chip analysis of co-precipitated RNAs indicates that PPR7 interacts with an unusually high number of different chloroplast transcripts.

Interestingly, the investigation of PPR7 knockdown strains suggests that the protein plays multiple roles in the expression of these RNAs. First, PPR7 seems to contribute to the stabilization of *rbcl*, *rpoC2*, *psbH*, and *tscA* transcripts. Binding sites for RNA stability factors usually lie in the 5' or 3' UTRs of their targets, where they act as barriers to the progression of exonucleases, but the resolution of our RIP-chip analysis does not allow us to

determine whether this is true also for PPR7. Remarkably, the putative PPR7 binding site on the *rpoC2* transcript is located within the intron-less coding region, which may imply that binding of PPR7 stabilizes this transcript by protecting an endonuclease-sensitive site.

As a second general function of PPR7, we suggest its involvement in the maturation of polycistronic mRNAs (*psbJ* and *atpA* gene clusters) as well as of 16S rRNA. In these cases, we observed abnormal accumulation of polycistronic transcripts often at the expense of processed forms in PPR7-depleted strains, but the specific role of the protein in RNA maturation remains unclear. It might recruit certain endonucleases or modify the structure of its targets to unmask a nuclease-sensitive sequence, as has been proposed for other PPR proteins (reviewed in Barkan and Small, 2014). High-resolution mapping of PPR7's binding sites and detailed RNA binding studies will be required to further elucidate its precise molecular impact on the identified target RNAs.

In all cases described above, transcript accumulation is only moderately affected in *iPPR7* strains. While this might be attributable to the presence of residual PPR7 protein, it could also indicate that PPR7 is only one of several protein factors that contribute to the stabilization of these transcripts. Other RNA binding proteins acting on the same transcripts could thus compensate for the absence of PPR7. At least in the case of *rbcl* and the *psbB/T/H* transcription unit, the factors MRL1 and MBB1, respectively, have been reported to be necessary for their stable accumulation (see above). Unfortunately, we were unable to identify PPR7 knockdown strains with less than 15% of the WT level. This may indicate the importance of PPR7 for cell survival, which would be compatible with the essential functions of some of PPR7's targets, e.g. the 16S rRNA or the  $\beta'$  subunit of the essential plastid RNA polymerase (Rochaix, 1995; Fischer et al., 1996). This idea is further supported by our inability to identify a PPR7 knockout mutant in an indexed library of *C. reinhardtii* insertional mutants (Gonzalez-Ballester et al., 2011; A.V. Bohne, A. Grossman, and J. Nickelsen, unpublished data). PPR7 is the most heavily expressed PPR gene in *Chlamydomonas*, which also suggests an essential role for its product.

The relatively broad range of PPR7 targets is not surprising when one considers that it contains only four PPR repeats. According to the predicted PPR code, which suggests that each PPR repeat recognizes one nucleotide, *Chlamydomonas* PPR7 would recognize at best four nucleotides of its target RNAs. Nevertheless, PPR7 shows some specificity for certain RNA targets and does not bind randomly to RNA, which leads us to assume that other proteins found with PPR7 in large RNP complexes (see Figure 2) confer further binding specificity. The positively charged C-terminal tail of PPR7 might also enhance binding to negatively charged RNA molecules (see Supplemental Figure 1).

So far, the recognition of three or more different RNA targets has been only described for certain PPR proteins involved in RNA editing (e.g. Hammani et al., 2009; Kim et al., 2009; Zehrmann et al., 2009). Often the specifically recognized sequences upstream of the respective editing sites are only partially or barely conserved, so the reason for a precise target recognition mechanism remains to be resolved. It was proposed that editing factors can

discriminate between purines and pyrimidines and that only certain specific nucleotides in the *cis*-acting elements are sufficient for high-affinity binding of a PPR protein (Hammani et al., 2009; Okuda and Shikanai, 2012). However, the specificity of these editing factors for multiple transcripts is most likely guaranteed by numerous PPR repeats while the RNA targeting mechanism of PPR7 should be clearly different.

Recently a novel PPR subfamily, the THA8 family, was described in higher plants, whose members are also very small and possess only four PPR motifs (Khrouchtchova et al., 2012). THA8 from maize, in contrast to PPRs investigated so far, exhibits only weak RNA binding activity and no specificity *in vitro*. Nevertheless, the protein specifically recognizes only two group II introns of *ycf3-2* and *trnA* transcripts *in vivo*, which also suggests that determinants for specific recognition of the two target RNAs are not provided directly by THA8 (Khrouchtchova et al., 2012). Note, however, that PPR7 and THA8 are not orthologous and that PPR7 is truly specific to green algae (Tourasse et al., 2013).

Interestingly, the same analysis revealed that the average number of repeats per PPR protein is in general lower in algae than in higher plants (7.7 versus 12.5). This indicates a generally lower specificity of these proteins based on the proposed recognition mechanism of RNA ligands described above. Because many of the functions of PPR proteins require tight binding to their RNA targets for the specificity, they would require a large number of highly specific proteins (there are 450 PPRs in *Arabidopsis*). It is clear that, if they acted by themselves, the 14 PPR proteins of *C. reinhardtii* could not control organellar mRNA metabolism in a gene-specific manner. In *Chlamydomonas*, the scarcity of PPRs might be compensated by the presence of other RNA binding proteins belonging to different repeat protein families such as the tetratricopeptide repeat (TPR) and, even more so, the many representatives of the octotricopeptide repeat (OPR) proteins (Boudreau et al., 2000; Eberhard et al., 2011; Rahire et al., 2012; Kleinknecht et al., 2014). In these families as well, it is likely that other cases will be reported of proteins with broader target specificity than is usually described. Historically, forward genetic studies focusing on mutants with highly specific phenotypes have led to the notion that target binding must be gene specific. The diverse functions of PPR7 identified in this study, and the observation that a substantial decrease in PPR7 level only mildly perturbs the stability or processing of its targets together point to another theme that may become more prominent as reverse genetic studies develop: broad specificity, multifunctionality, and cooperation within a network of interacting RNA stability, maturation, and translation factors.

## METHODS

### Algal Strains and Culture Conditions

Algal strains were grown at 23°C in Tris–acetate–phosphate medium under moderate (ML, 30  $\mu\text{E}/\text{m}^2/\text{s}$ ) or higher (HL, 100  $\mu\text{E}/\text{m}^2/\text{s}$ ) light or in darkness (D) (Gorman and Levine, 1965). Liquid cultures were supplemented with 1% sorbitol. For photoautotrophic growth, cells were cultured in high-salt minimal medium HSM (Sager and Granick, 1953). As the WT *C. reinhardtii* strain, we used the cell-wall-deficient strain CC406. For green fluorescent protein (GFP) import studies and the generation of RNAi strains, the expression strain UVM4 (Neupert et al., 2009) was used.

### GFP Import Studies

Cloning, selection of transformants, and GFP import studies were essentially performed as described in Bohne et al. (2013). For expression of a PPR7-GFP fusion protein, the coding sequence of the N-terminal amino acids 1–72, including the transit peptide predicted by ChloroP (<http://www.cbs.dtu.dk/services/ChloroP/>; Emanuelsson et al., 1999), was PCR-amplified from cDNA with the primer pair PPR7 TP Fw/PPR7 TP Rv (Supplemental Table 3) introducing 5' and 3' *NdeI* sites. The *NdeI* fragment was then inserted into pBC1-CrGFP (pJR38, Neupert et al., 2009) to generate pBC1-TP-PPR7-CrGFP. This construct was transformed into UVM4, and positive transformants were analyzed by laser scanning confocal fluorescence microscopy. As a control, the pBC1-CrGFP vector was directly transformed into UVM4 for cytosolic GFP expression. Mitochondria were stained with MitoTracker Red CMXRos (Molecular Probes).

### Production of Antiserum against PPR7

A PPR7 DNA sequence encoding the C-terminal amino acids 166–220 was PCR-amplified from cDNA using the primer pair PPR7fw/rev (Supplemental Table 3). The PCR product was inserted into the expression vector pGEX4T1 (GE Healthcare) via primer-introduced *BamHI* and *XhoI* restriction sites, overexpressed in *Escherichia coli* BL21 cells, and purified according to the manufacturer's protocol using glutathione-Sepharose 4B (GE Healthcare). A polyclonal antiserum was produced by immunizing rabbits with the purified GST-tagged protein (Biogenes). Crude antiserum was affinity purified by binding to Western blots, and eluting the antibodies from the target band with glycine buffer (0.1 M glycine–HCl, pH 2.7). The acidic solution was then neutralized by adding 1/10 volume of 1 M Tris–HCl, pH 8. To stabilize the antibody, sodium azide and bovine serum albumin were added to a final concentration of 5 mM and 1 mg/ml, respectively.

### RNA Preparation and RNA Blot Analysis

Liquid cultures of *C. reinhardtii* strains under investigation were grown in the light (100  $\mu\text{E}/\text{m}^2/\text{s}$ ) and harvested at early log phase ( $\sim 1 \times 10^6$  to  $2 \times 10^6$  cells/ml) by centrifugation at 1100 g and 4°C for 6 min. Total RNA was extracted using TRI reagent (Sigma), according to the manufacturer's instructions. RNAs were subjected to Northern blot analysis using standard methods. Digoxigenin-labeled DNA probes were generated by PCR using primers listed in Supplemental Table 3.

### Protein Preparations

For isolation of total protein extracts, cells were grown in TAPS medium to a density of  $\sim 2 \times 10^6$  to  $3 \times 10^6$  cells/ml, harvested as before, and resuspended in 2 $\times$  lysis buffer (120 mM KCl, 0.4 mM EDTA, 20 mM Tricine pH 7.8, 5 mM  $\beta$ -mercaptoethanol, 0.2% Triton X-100, and Roche Complete Mini protease inhibitors).

For isolation of soluble proteins, cell pellets were resuspended in hypotonic solution (10 mM Tricine/KOH pH 7.8, 10 mM EDTA, 5 mM  $\beta$ -mercaptoethanol, and Roche Complete Mini protease inhibitors) and lysed by sonication. Insoluble material was pelleted by centrifugation (10 000 g, 4°C, 10 min), and the supernatant served as the soluble protein extract.

For the preparation of chloroplast proteins, chloroplasts were isolated from a cell wall-deficient WT strain (*cw15*) on a discontinuous Percoll gradient as described by Zerges and Rochaix (1998). To obtain total chloroplast proteins, chloroplasts were lysed directly in breaking buffer (120 mM KCl, 0.4 mM EDTA, 20 mM Tricine pH 7.8, 5 mM  $\beta$ -mercaptoethanol, 0.2% Triton X-100, and Roche Complete Mini protease inhibitors).

Fractionation of chloroplasts into stroma and thylakoid fractions was carried out as described by Ossenbühl and Nickelsen (2000). In brief, the pelleted chloroplasts were osmotically lysed in reducing hypotonic buffer (10 mM Tricine/KOH pH 7.8, 10 mM EDTA, 5 mM  $\beta$ -mercaptoethanol, and Roche Complete Mini protease inhibitors), and

insoluble material was removed by ultracentrifugation through a 1 M sucrose cushion for 30 min at 100 000 *g*. The supernatant obtained served as the stromal fraction and the pellet as the crude thylakoid fraction for immunoblot analysis. For SEC and co-immunoprecipitation experiments, chloroplasts were lysed in non-reducing hypotonic buffer.

For isolation of mitochondrial proteins, mitochondria were isolated from the *cw15* strain as described by Eriksson et al. (1995). Purified mitochondria were disrupted by sonication and subjected to immunoblot analysis.

### SEC of Stromal Proteins

SEC was carried out essentially as described by Bohne et al. (2013). Stromal extracts were concentrated in 3-kDa-cutoff Amicon Ultra filtration devices (Millipore), with or without 400 U RNase One/mg protein (Promega). Samples were loaded through an SW guard column onto a 2.15 × 30-cm G4000SW column (Tosoh), and elution was performed at 4°C with SEC buffer (50 mM KCl, 5 mM MgCl<sub>2</sub>, 5 mM ε-aminocaproic acid, and 20 mM Tricine/KOH pH 7.5) at a flow rate of 2 ml/min. The eluted fractions obtained were further concentrated to about 70 μl using 10-kDa-cutoff Amicon Ultra devices (Millipore), and aliquots of each fraction were subjected to immunoblotting.

### SDS-PAGE and Immunoblot Analysis

SDS-PAGE and immunoblot analysis were performed using standard procedures. Protein concentrations were determined using the Bradford (C. Roth) assay following the manufacturer's instructions.

### Microarray Design and Hybridization of Co-Immunoprecipitated RNA to Gene Chips

For co-immunoprecipitation of RNA associated with PPR7 protein, stromal extracts were prepared as described above in the presence of 0.5 mg/ml yeast tRNA and 250 U/ml RNase inhibitor (Fermentas). PPR7 antibody was incubated with stroma for 45 min, followed by a 30-min incubation with 50 μl of Dynabead-coupled protein G (Invitrogen) that had been pre-equilibrated with co-immunoprecipitation buffer (150 mM NaCl, 20 mM Tris-HCl pH 7.5, 10 mM MgCl<sub>2</sub>, and 0.5% [v/v] Nonidet P-40). An aliquot (1/10 volume) of supernatant stroma was taken for immunoblot analysis and the rest was used for RNA extraction. The beads were washed five times with co-immunoprecipitation buffer (+5 μg/ml aprotinin and 400 U/ml RNase inhibitor [Fermentas]) and resuspended in 180 μl of the same buffer. RNA was extracted by the phenol/chloroform method from supernatant and beads after the addition of SDS to 0.5%.

Labeling of RNA that co-purified with PPR7 was carried out as described previously (Schmitz-Linneweber et al., 2005) using the ULS labeling kit (Kreatech). A microarray was designed with 166 overlapping PCR fragments representing the complete *C. reinhardtii* chloroplast genome and 15 overlapping PCR fragments representing the complete mitochondrial genome. Total DNA extracted from *C. reinhardtii* cells served as the template for PCRs. PCR product positions and primers used for amplification are listed in Supplemental Table 2. PCR products were numbered (ID) according to their positions in the *C. reinhardtii* chloroplast and mitochondrial genome sequences (accession numbers BK000554 for chloroplast and U03843 for mitochondrial probes). Each product was spotted in multiple copies using an Omnigridd Accent spotting device (GeneMachines). For each microarray slide, PCR products were spotted in two areas. In area A, 12 replicates per PCR product were spotted, whereas in area B only 6 replicates were spotted. Area A was hybridized with RNA from immunoprecipitations using α-PPR7 antibody, whereas area B was hybridized with RNA from parallel immunoprecipitations using pre-immune serum as control. This parallel processing of experiment and control allowed maximum comparability during hybridization and subsequent washings. RNA labeling, hybridization of RNA to the *C. reinhardtii* chloroplast microarray, and data analysis were carried out as reported previously, using a Scanarray Gx

microarray scanner (Perkin Elmer) and the Genepix Pro 6.0 analysis software (Axon; Schmitz-Linneweber et al., 2005). We performed four replicate RIP-chip experiments for both the immunoprecipitation of PPR7 and the mock control precipitation using pre-immune serum.

### cDNA Synthesis and RT-PCR

Reverse transcription (RT) was performed with 100–500 ng of RNA co-immunoprecipitated with PPR7 as described above, using MonsterScript Reverse Transcriptase (Epicentre) and gene-specific primers according to the supplier's instructions. RNase-free DNase I (Promega) was used to remove DNA prior to RT-PCRs. For semi-quantitative RT-PCR, 20 cycles were used to amplify specific sequences. All primers used are listed in Supplemental Table 3.

### Generation of PPR7 RNAi Strains

RNAi strains were generated by the method of Rohr et al. (2004), and selected and cultured as described by Bohne et al. (2013). Sequences of primer pairs iPPR7-400a/iPPR7-400b and iPPR7-400a/iPPR7-600c used for cloning inverted repeats into the EcoRI site of the NE537 vector (Rohr et al., 2004) are listed in Supplemental Table 3. To generate the control strain, the empty NE537 vector was transformed into UVM4.

### Spectroscopy and Fluorescence Measurements

The JTS-10 spectrophotometer (Biologic, Grenoble, France) was used for *in vivo* spectroscopy measurement. Cells grown in 100 ml TAP were harvested in the mid-exponential phase and resuspended in 2 ml HEPES (20 mM, pH 7.2) containing 20% (w/w) Ficoll. They were kept in the dark with vigorous shaking for 20 min before measurements. Fluorescence was excited with a green LED (520 nm) and measured in the near far red. Fv/Fm was calculated as the average over six experiments at various light intensities. PSI/PSII ratios were evaluated from the amplitude of the ECS signal measured in the presence or absence of the PSII inhibitors DCMU (20 μM) and hydroxylamine (1 mM) according to Joliot and Delosme (1974).

### SUPPLEMENTAL INFORMATION

Supplemental Information is available at *Molecular Plant Online*.

### FUNDING

This work was supported by a grant from the Deutsche Forschungsgemeinschaft to J.N. (Grant Ni390/4-2). A.J. was supported by a HEC/DAAD Postgraduate programme (A/07/96824). C.S.L. wishes to acknowledge support by the Deutsche Forschungsgemeinschaft (Grant SCHM 1698/2-2). O.V. acknowledges support from the French Initiative d'Excellence grant DYNAMO (ANR-11-LABX-0011-01). J.N. and O.V. thank the bilateral German/French academic exchange program PROCOPPE, sponsored by the German DAAD (Deutscher Akademischer Austauschdienst - German Academic Exchange Service) and the French MAE (Ministere des Affaires Etrangères - Ministry for Foreign Affairs).

### ACKNOWLEDGMENTS

We thank K. Findeisen, R. Modrozynski, and Marlene Teubner for skilled technical assistance, and Michael Schroda for kindly providing the anti-HSP70B antibody. No conflict of interest declared.

Received: April 30, 2014

Revised: November 10, 2014

Accepted: November 24, 2014

Published: December 17, 2014

### REFERENCES

Ban, T., Ke, J., Chen, R., Gu, X., Tan, M.H.E., Zhou, X.E., Kang, Y., Melcher, K., Zhu, J.K., and Xu, H.E. (2013). Structure of a PLS-class pentatricopeptide repeat protein provides insights into mechanism of RNA recognition. *J. Biol. Chem.* **288**:31540–31548.

- Barkan, A.** (2011). Expression of plastid genes: organelle-specific elaborations on a prokaryotic scaffold. *Plant Physiol.* **155**:1520–1532.
- Barkan, A., and Small, I.** (2014). Pentatricopeptide repeat proteins in plants. *Annu. Rev. Plant Biol.* **65**:415–442.
- Barkan, A., Rojas, M., Fujii, S., Yap, A., Chong, Y.S., Bond, C.S., and Small, I.** (2012). A combinatorial amino acid code for RNA recognition by pentatricopeptide repeat proteins. *PLoS Genet.* **8**:e1002910.
- Bohne, A.V., Schwarz, C., Schottkowski, M., Lidschreiber, M., Piotrowski, M., Zerges, W., and Nickelsen, J.** (2013). Reciprocal regulation of protein synthesis and carbon metabolism for thylakoid membrane biogenesis. *PLoS Biol.* **11**:e1001482.
- Boudreau, E., Nickelsen, J., Lemaire, S.D., Ossenbühl, F., and Rochaix, J.D.** (2000). The Nac2 gene of *Chlamydomonas* encodes a chloroplast TPR-like protein involved in *psbD* mRNA stability. *EMBO J.* **19**:3366–3376.
- Boulouis, A., Raynaud, C., Bujaldon, S., Aznar, A., Wollman, F.A., and Choquet, Y.** (2011). The nucleus-encoded trans-acting factor MCA1 plays a critical role in the regulation of cytochrome *f* synthesis in *Chlamydomonas* chloroplasts. *Plant Cell* **23**:333–349.
- Castruita, M., Casero, D., Karpowicz, S.J., Kropat, J., Vieler, A., Hsieh, S.I., Yan, W., Cokus, S., Loo, J.A., Benning, C., et al.** (2011). Systems biology approach in *Chlamydomonas* reveals connections between copper nutrition and multiple metabolic steps. *Plant Cell* **23**:1273–1292.
- Choquet, Y., Wostrickoff, K., Rimbault, B., Zito, F., Girard-Bascou, J., Drapier, D., and Wollman, F.A.** (2001). Assembly-controlled regulation of chloroplast gene translation. *Biochem. Soc. Trans.* **29**:421–426.
- Drapier, D., Suzuki, H., Levy, H., Rimbault, B., Kindle, K.L., Stern, D.B., and Wollman, F.A.** (1998). The chloroplast *atpA* gene cluster in *Chlamydomonas reinhardtii*. Functional analysis of a polycistronic transcription unit. *Plant Physiol.* **117**:629–641.
- Drapier, D., Rimbault, B., Vallon, O., Wollman, F.A., and Choquet, Y.** (2007). Intertwined translational regulations set uneven stoichiometry of chloroplast ATP synthase subunits. *EMBO J.* **26**:3581–3591.
- Eberhard, S., Loiselay, C., Drapier, D., Bujaldon, S., Girard-Bascou, J., Kuras, R., Choquet, Y., and Wollman, F.A.** (2011). Dual functions of the nucleus-encoded factor TDA1 in trapping and translation activation of *atpA* transcripts in *Chlamydomonas reinhardtii* chloroplasts. *Plant J.* **67**:1055–1066.
- Emanuelsson, O., Nielsen, H., and von Heijne, G.** (1999). ChloroP—a neural network-based method for predicting chloroplast transit peptides and their cleavage sites. *Protein Sci.* **8**:978–984.
- Emanuelsson, O., Nielsen, H., Brunak, S., and von Heijne, G.** (2000). Predicting subcellular localization of proteins based on their N-terminal amino acid sequence. *J. Mol. Biol.* **300**:1005–1016.
- Eriksson, M., Gardstrom, P., and Samuelsson, G.** (1995). Isolation, purification, and characterization of mitochondria from *Chlamydomonas reinhardtii*. *Plant Physiol.* **107**:479–483.
- Fischer, N., Stampacchia, O., Redding, K., and Rochaix, J.D.** (1996). Selectable marker recycling in the chloroplast. *Mol. Gen. Genet.* **251**:373–380.
- Fischer, N., Boudreau, E., Hippler, M., Drepper, F., Haehnel, W., and Rochaix, J.D.** (1999). A large fraction of Psaf is nonfunctional in photosystem I complexes lacking the Psaj subunit. *Biochemistry* **38**:5546–5552.
- Fisk, D.G., Walker, M.B., and Barkan, A.** (1999). Molecular cloning of the maize gene *crp1* reveals similarity between regulators of mitochondrial and chloroplast gene expression. *EMBO J.* **18**:2621–2630.
- Fujii, S., and Small, I.** (2011). The evolution of RNA editing and pentatricopeptide repeat genes. *New Phytol.* **191**:37–47.
- Fujii, S., Bond, C.S., and Small, I.D.** (2011). Selection patterns on restorer-like genes reveal a conflict between nuclear and mitochondrial genomes throughout angiosperm evolution. *Proc. Natl. Acad. Sci. USA* **108**:1723–1728.
- Fujii, S., Sato, N., and Shikanai, T.** (2013). Mutagenesis of individual pentatricopeptide repeat motifs affects RNA binding activity and reveals functional partitioning of *Arabidopsis* PROTON GRADIENT REGULATION3. *Plant Cell* **25**:3079–3088.
- Gillman, J.D., Bentolila, S., and Hanson, M.R.** (2007). The petunia restorer of fertility protein is part of a large mitochondrial complex that interacts with transcripts of the CMS-associated locus. *Plant J.* **49**:217–227.
- Glanz, S., Jacobs, J., Kock, V., Mishra, A., and Kück, U.** (2012). Raa4 is a trans-splicing factor that specifically binds chloroplast *tscA* intron RNA. *Plant J.* **69**:421–431.
- Goldschmidt-Clermont, M., Choquet, Y., Girard-Bascou, J., Michel, F., Schirmer-Rahire, M., and Rochaix, J.D.** (1991). A small chloroplast RNA may be required for trans-splicing in *Chlamydomonas reinhardtii*. *Cell* **65**:135–143.
- Gonzalez-Ballester, D., Pootakham, W., Mus, F., Yang, W., Catalanotti, C., Magneschi, L., de Montaigu, A., Higuera, J., Prior, M., Galvan, A., et al.** (2011). Reverse genetics in *Chlamydomonas*: a platform for isolating insertional mutants. *Plant Meth.* **7**:24.
- Gorman, D.S., and Levine, R.P.** (1965). Cytochrome *f* and plastocyanin: their sequence in the photosynthetic electron transport chain of *Chlamydomonas reinhardtii*. *Proc. Natl. Acad. Sci. USA* **54**:1665–1669.
- Hahn, D., Nickelsen, J., Hackert, A., and Kueck, U.** (1998). A single nuclear locus is involved in both chloroplast RNA trans-splicing and 3' end processing. *Plant J.* **15**:575–581.
- Hammani, K., Okuda, K., Tanz, S.K., Chateigner-Boutin, A.L., Shikanai, T., and Small, I.** (2009). A study of new *Arabidopsis* chloroplast RNA editing mutants reveals general features of editing factors and their target sites. *Plant Cell* **21**:3686–3699.
- Hammani, K., Bonnard, G., Bouchoucha, A., Gobert, A., Pinker, F., Salinas, T., and Giegé, P.** (2014). Helical repeats modular proteins are major players for organelle gene expression. *Biochimie* **100**:141–150.
- Holloway, S.P., and Herrin, D.L.** (1998). Processing of a composite large subunit rRNA: studies with *Chlamydomonas* mutants deficient in maturation of the 23S-like rRNA. *Plant Cell* **10**:1193–1206.
- Jacobs, J., Glanz, S., Bunse-Graßmann, A., Kruse, O., and Kück, U.** (2010). RNA trans-splicing: identification of components of a putative chloroplast spliceosome. *Eur. J. Cell Biol.* **89**:932–939.
- Johnson, X.** (2011). Manipulating RuBisCO accumulation in the green alga, *Chlamydomonas reinhardtii*. *Plant Mol. Biol.* **76**:397–405.
- Johnson, C.H., and Schmidt, G.W.** (1993). The *psbB* gene cluster of the *Chlamydomonas reinhardtii* chloroplast: sequence and transcriptional analyses of *psbN* and *psbH*. *Plant Mol. Biol.* **22**:645–658.
- Johnson, X., Wostrickoff, K., Finazzi, G., Kuras, R., Schwarz, C., Bujaldon, S., Nickelsen, J., Stern, D.B., Wollman, F.A., and Vallon, O.** (2010). MRL1, a conserved pentatricopeptide repeat protein, is required for stabilization of *rbcL* mRNA in *Chlamydomonas* and *Arabidopsis*. *Plant Cell* **22**:234–248.
- Joliot, P., and Delosme, R.** (1974). Flash-induced 519 nm absorption change in green algae. *Biochim. Biophys. Acta* **357**:267–284.
- Khrouchtchova, A., Monde, R.A., and Barkan, A.** (2012). A short PPR protein required for the splicing of specific group II introns in angiosperm chloroplasts. *RNA* **18**:1197–1209.

- Kim, S.R., Yang, J.I., Moon, S., Ryu, C.H., An, K., Kim, K.M., Yim, J., and An, G. (2009). Rice OGR1 encodes a pentatricopeptide repeat-DYW protein and is essential for RNA editing in mitochondria. *Plant J.* **59**:738–749.
- Kleinknecht, L., Wang, F., Stübe, R., Philippar, K., Nickelsen, J., and Bohne, A.V. (2014). RAP, the sole octotricopeptide repeat protein in *Arabidopsis*, is required for chloroplast 16S rRNA maturation. *Plant Cell* **26**:777–787.
- Kobayashi, K., Kawabata, M., Hisano, K., Kazama, T., Matsuoka, K., Sugita, M., and Nakamura, T. (2012). Identification and characterization of the RNA binding surface of the pentatricopeptide repeat protein. *Nucleic Acids Res.* **40**:2712–2723.
- Lightowers, R.N., and Chrzanowska-Lightowers, Z.M.A. (2008). PPR (pentatricopeptide repeat) proteins in mammals: important aids to mitochondrial gene expression. *Biochem. J.* **416**:e5–e6.
- Lipinski, K.A., Puchta, O., Surandranath, V., Kudla, M., and Golik, P. (2011). Revisiting the yeast PPR proteins—application of an iterative hidden Markov model algorithm reveals new members of the rapidly evolving family. *Mol. Biol. Evol.* **28**:2935–2948.
- Liu, X.Q., Gillham, N.W., and Boynton, J.E. (1989). Chloroplast ribosomal protein gene *rps12* of *Chlamydomonas reinhardtii*. Wild-type sequence, mutation to streptomycin resistance and dependence, and function in *Escherichia coli*. *J. Biol. Chem.* **264**:16100–16108.
- Loiselay, C., Gumpel, N.J., Girard-Bascou, J., Watson, A.T., Purton, S., Wollman, F.A., and Choquet, Y. (2008). Molecular identification and function of cis- and trans-acting determinants for *petA* transcript stability in *Chlamydomonas reinhardtii* chloroplasts. *Mol. Cell Biol.* **28**:5529–5542.
- Lurin, C., Andres, C., Aubourg, S., Bellaoui, M., Bitton, F., Bruyere, C., Caboche, M., Debast, C., Gualberto, J., Hoffmann, B., et al. (2004). Genome-wide analysis of *Arabidopsis* pentatricopeptide repeat proteins reveals their essential role in organelle biogenesis. *Plant Cell* **16**:2089–2103.
- Majeran, W., Olive, J., Drapier, D., Vallon, O., and Wollman, F.A. (2001). The light sensitivity of ATP synthase mutants of *Chlamydomonas reinhardtii*. *Plant Physiol.* **126**:421–433.
- Meierhoff, K., Felder, S., Nakamura, T., Bechtold, N., and Schuster, G. (2003). HCF152, an *Arabidopsis* RNA binding pentatricopeptide repeat protein involved in the processing of chloroplast *psbB-psbT-psbH-petB-petD* RNAs. *Plant Cell* **15**:1480–1495.
- Monod, C., Goldschmidt-Clermont, M., and Rochaix, J.D. (1992). Accumulation of chloroplast *psbB* RNA requires a nuclear factor in *Chlamydomonas reinhardtii*. *Mol. Gen. Genet.* **231**:449–459.
- Nakamura, T., Meierhoff, K., Westhoff, P., and Schuster, G. (2003). RNA-binding properties of HCF152, an *Arabidopsis* PPR protein involved in the processing of chloroplast RNA. *Eur. J. Biochem.* **270**:4070–4081.
- Neupert, J., Karcher, D., and Bock, R. (2009). Generation of *Chlamydomonas* strains that efficiently express nuclear transgenes. *Plant J.* **57**:1140–1150.
- O'Connor, H.E., Ruffle, S.V., Cain, A.J., Deak, Z., Vass, I., Nugent, J.H.A., and Purton, S. (1998). The 9-kDa phosphoprotein of photosystem: II. Generation and characterisation of *Chlamydomonas* mutants lacking PSII-H and a site-directed mutant lacking the phosphorylation site. *Biochim. Biophys. Acta* **1364**:63–72.
- Okuda, K., and Shikanai, T. (2012). A pentatricopeptide repeat protein acts as a site-specificity factor at multiple RNA editing sites with unrelated cis-acting elements in plastids. *Nucleic Acids Res.* **40**:5052–5064.
- Ossenbühl, F., and Nickelsen, J. (2000). Cis- and trans-acting determinants for translation of *psbD* mRNA in *Chlamydomonas reinhardtii*. *Mol. Cell. Biol.* **20**:8134–8142.
- Pfalz, J., Bayraktar, O.A., Prikryl, J., and Barkan, A. (2009). Site-specific binding of a PPR protein defines and stabilizes 5' and 3' mRNA termini in chloroplasts. *EMBO J.* **28**:2042–2052.
- Prikryl, J., Rojas, M., Schuster, G., and Barkan, A. (2011). Mechanism of RNA stabilization and translational activation by a pentatricopeptide repeat protein. *Proc. Natl. Acad. Sci. USA* **108**:415–420.
- Rahire, M., Laroche, F., Cerutti, L., and Rochaix, J.D. (2012). Identification of an OPR protein involved in the translation initiation of the PsaB subunit of photosystem I. *Plant J.* **72**:652–661.
- Raynaud, C., Loiselay, C., Wostrikoff, K., Kuras, R., Girard-Bascou, J., Wollman, F.A., and Choquet, Y. (2007). Evidence for regulatory function of nucleus-encoded factors on mRNA stabilization and translation in the chloroplast. *Proc. Natl. Acad. Sci. USA* **104**:9093–9098.
- Rochaix, J.D. (1995). *Chlamydomonas reinhardtii* as the photosynthetic yeast. *Annu. Rev. Genet.* **29**:209–230.
- Rochaix, J.D. (1996). Post-transcriptional regulation of chloroplast gene expression in *Chlamydomonas reinhardtii*. *Plant Mol. Biol.* **32**:327–341.
- Rohr, J., Sarkar, N., Balenger, S., Jeong, B.R., and Cerutti, H. (2004). Tandem inverted repeat system for selection of effective transgenic RNAi strains in *Chlamydomonas*. *Plant J.* **40**:611–621.
- Rymarquis, L.A., Higgs, D.C., and Stern, D.B. (2006). Nuclear suppressors define three factors that participate in both 5' and 3' end processing of mRNAs in *Chlamydomonas* chloroplasts. *Plant J.* **46**:448–461.
- Sager, R., and Granick, S. (1953). Nutritional studies with *Chlamydomonas reinhardtii*. *Ann. N. Y. Acad. Sci.* **56**:831–838.
- Salvador, M., Klein, U., and Bogorad, L. (1993). 5' sequences are important positive and negative determinants of the longevity of *Chlamydomonas* chloroplast gene transcripts. *Proc. Natl. Acad. Sci. USA* **90**:1556–1560.
- Schmitz-Linneweber, C., and Small, I. (2008). Pentatricopeptide repeat proteins: a socket set for organelle gene expression. *Trends Plant Sci.* **13**:663–670.
- Schmitz-Linneweber, C., Williams-Carrier, R., and Barkan, A. (2005). RNA immunoprecipitation and microarray analysis show a chloroplast pentatricopeptide repeat protein to be associated with the 5' region of mRNAs whose translation it activates. *Plant Cell* **17**:2791–2804.
- Schmitz-Linneweber, C., Williams-Carrier, R.E., Williams-Voelker, P.M., Kroeger, T.S., Vichas, A., and Barkan, A. (2006). A pentatricopeptide repeat protein facilitates the trans-splicing of the maize chloroplast *rps12* pre-mRNA. *Plant Cell* **18**:2650–2663.
- Shikanai, T., and Fujii, S. (2013). Function of PPR proteins in plastid gene expression. *RNA Biol.* **10**:1446–1456.
- Small, I., Peeters, N., Legeai, F., and Lurin, C. (2004). Predotar: a tool for rapidly screening proteomes for N-terminal targeting sequences. *Proteomics* **4**:1581–1590.
- Sommer, F., Hippler, M., Biehler, K., Fischer, N., and Rochaix, J.D. (2003). Comparative analysis of photosensitivity in photosystem I donor and acceptor side mutants of *Chlamydomonas reinhardtii*. *Plant Cell Environ.* **26**:1881–1892.
- Spreitzer, R.J., and Mets, L. (1981). Photosynthesis-deficient mutants of *Chlamydomonas reinhardtii* with associated light-sensitive phenotypes. *Plant Physiol.* **67**:565–569.
- Stern, D.B., Goldschmidt-Clermont, M., and Hanson, M.R. (2010). Chloroplast RNA metabolism. *Annu. Rev. Plant Biol.* **61**:125–155.

- Takenaka, M., Zehrmann, A., Brennicke, A., and Graichen, K.** (2013). Improved computational target site prediction for pentatricopeptide repeat RNA editing factors. *PLoS One* **8**:e65343.
- Tardif, M., Atteia, A., Specht, M., Cogne, G., Rolland, N., Brugière, S., Hippler, M., Ferro, M., Bruley, C., Peltier, G., et al.** (2012). PredAlgo: a new subcellular localization prediction tool dedicated to green algae. *Mol. Biol. Evol.* **29**:3625–3639.
- Tourasse, N.J., Choquet, Y., and Vallon, O.** (2013). PPR proteins of green algae. *RNA Biol.* **10**:1526–1542.
- Urzica, E.I., Casero, D., Yamasaki, H., Hsieh, S.I., Adler, L.N., Karpowicz, S.J., Blaby-Haas, C.E., Clarke, S.G., Loo, J.A., Pellegrini, M., et al.** (2012). Systems and trans-system level analysis identifies conserved iron deficiency responses in the plant lineage. *Plant Cell* **24**:3921–3948.
- Yagi, Y., Hayashi, S., Kobayashi, K., Hirayama, T., and Nakamura, T.** (2013). Elucidation of the RNA recognition code for pentatricopeptide repeat proteins involved in organelle RNA editing in plants. *PLoS One* **8**:e57286.
- Yin, P., Li, Q., Yan, C., Liu, Y., Liu, J., Yu, F., Wang, Z., Long, J., He, J., Wang, H.W., et al.** (2013). Structural basis for the modular recognition of single-stranded RNA by PPR proteins. *Nature* **504**:168–171.
- Zehrmann, A., Verbitskiy, D., van der Merwe, J.A., Brennicke, A., and Takenaka, M.** (2009). A DYW domain-containing pentatricopeptide repeat protein is required for RNA editing at multiple sites in mitochondria of *Arabidopsis thaliana*. *Plant Cell* **21**:558–567.
- Zerges, W., and Rochaix, J.-D.** (1998). Low density membranes are associated with RNA-binding proteins and thylakoids in the chloroplast of *Chlamydomonas reinhardtii*. *J. Cell Biol.* **140**:101–110.
- Zhelyazkova, P., Hammani, K., Rojas, M., Voelker, R., Vargas-Suárez, M., Börner, T., and Barkan, A.** (2012). Protein-mediated protection as the predominant mechanism for defining processed mRNA termini in land plant chloroplasts. *Nucleic Acids Res.* **40**:3092–3105.